Overview of the CHILD Model

Version 2.0

Gregory E. Tucker[1], Nicole M. Gasparini, Rafael L. Bras, and Stephen T. Lancaster

Department of Civil and Environmental Engineering
Massachusetts Institute of Technology
Cambridge, MA 02139

Part I-B of final technical report submitted to U.S. Army Corps of Engineers
Construction Engineering Research Laboratory (USACERL)
by Gregory E. Tucker, Nicole M. Gasparini, Rafael L. Bras, and Stephen T. Lancaster
in fulfillment of contract number DACA88-95-C-0017

April, 1999

1. To whom correspondence should be addressed: Dept. of Civil & Environmental Engineering, MIT Room 48-429, Cambridge, MA 02139, ph. (617) 252-1607, fax (617) 253-7475, email gtucker@mit.edu

Overview of the CHILD Model

The CHILD model simulates landscape evolution by tracking the passage of water and sediment across an irregular lattice of points that represents the landscape surface. Figure 1 shows

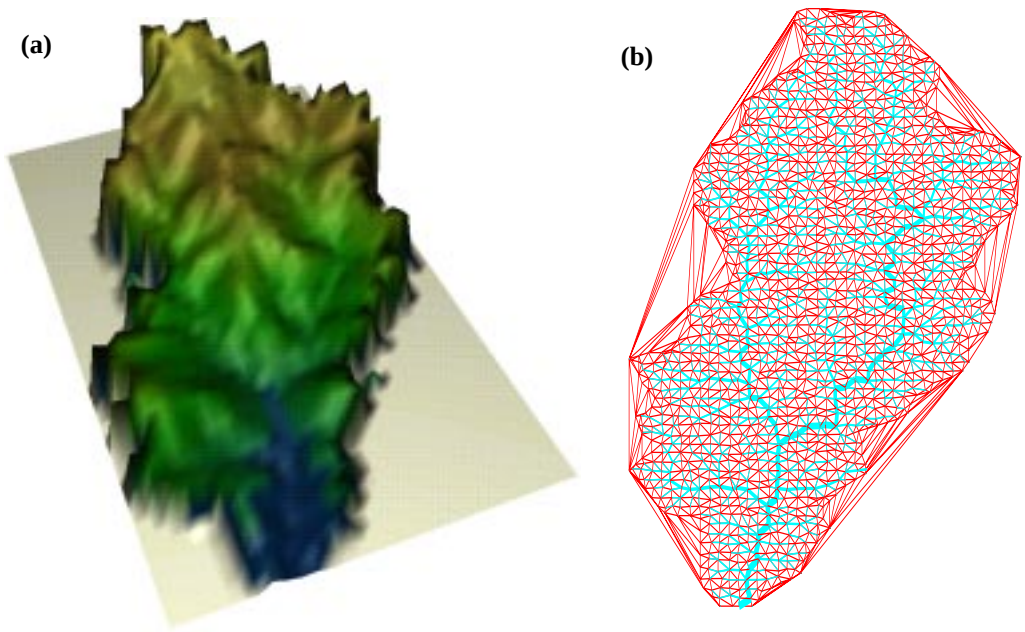

FIGURE 1. Drainage basin simulated using the CHILD model. (a) Perspective view of landscape. (For graphical display purposes, the mesh has been interpolated onto a regular grid. Visualization is from the SG3D module of GRASS.) (b) Plan view of drainage network and irregular mesh. The catchment outline is that of the Forsyth Creek watershed, Fort Riley, Kansas, and represents an area of about 11.5 km^2.

a typical simulation, highlighting the drainage networks that form naturally when converging flow excavates valleys and leads to further flow convergence. The model tracks a number of basic state variables that determine the depth of erosion or deposition at each point during a given iteration, including elevation, slope, drainage area, and surface runoff rate (Figure 1). The model also adds a three-dimensional component by tracking layers of deposited material at each point. Data associated with each layer include vertical thickness, time of deposition, erodibility, grain size composition, exposure age, and layer type (whether bedrock or regolith).

In generic mathematical terms, the model can be expressed by the following equation:

$$\frac{\partial z}{\partial t} = U([x, y, t]) - F(Q, S, [Q_s, C, V, D_g, \tau_{bk}]) - H(z) + D_{OB} + D_E \quad (1)$$

where z is surface elevation, t is time, and terms in brackets [] denote optional dependencies. The first term, $U()$, represents tectonic uplift (or equivalently, baselevel lowering), which may vary in time and space. The second term, $F()$, represents runoff erosion, and is a function of the runoff rate, Q, surface slope in the direction of flow, S, and optionally also of sediment flux, Q_s, and grain size composition of the substrate, D_g. No explicit distinction is made between erosion by overland flow and by fully channelized flow. The surface runoff rate, Q, is a function of drainage area, A, and optionally of slope, S (which can influence the likelihood of surface saturation and therefore of runoff production). Surface runoff can be modeled using a series of random storm events, or it can be modeled as a constant runoff rate that represents an average effective geomorphic event. Note that the runoff erosion term may also include the effects of lateral channel erosion, which is a function of local stream-bank shear stress, τ_{bk}. The third term, $H()$, represents sediment transport by hillslope processes such as soil creep, raindrop impact, and landsliding. In the present version of the model, hillslope transport depends solely on local topography; however, future versions may incorporate landsliding and its dependence on soil pore pressure (see Tucker and Bras, 1998). The fourth and fifth terms represent overbank deposition during floods and eolian deposition, respectively (these and any other terms may of course be zero in any particular application).

To compute the effects of these different processes, the model iterates through a series of discrete storm events and interstorm periods. These storm events can be modeled stochastically,

with the intensity and duration of each chosen at random from a distribution, or they may be uniform, in which case the storm properties represent a geomorphically "average" event (this is the assumption made in most previous models [e.g., Ahnert, 1976; Kirkby, 1987; Willgoose et al., 1991; Howard, 1994; Tucker and Slingerland, 1994; Moglen and Bras, 1995]).

The model provides considerable flexibility in the way that each of the process terms are modeled. Implementation of the various processes within the model is diagrammed in the form of a flow chart in Figure 2. The component process models are summarized below. Further discussion of many of these components is provided in later chapters.

Simulation Mesh: Generation and Dynamic Updating

The irregular mesh used in the model is described in detail by Tucker et al. (1999) (see Section I-C), but a brief overview now will help to clarify some of the concepts that follow. The model domain consists of a set of points N that are connected to form a mesh of triangles (Figure 3). Elevation, drainage area, and other state variables are computed at the points rather than within the triangles (in other words, the model uses a finite-difference rather than a finite-element approach). Points (or nodes) are connected using the Delaunay triangulation, which is the (generally) unique set of triangles that connect a given set of points in such a way that a circle passing through the three points in any triangle will contain no other points. Each node N_i is associated with a surrounding Voronoi cell (or Voronoi region). The Voronoi cell for a node N_i is the region within which any arbitrary point Q would be closer to N_i than to any other node on the grid. The boundaries between Voronoi cells are lines of equal distance between adjacent grid points. Each

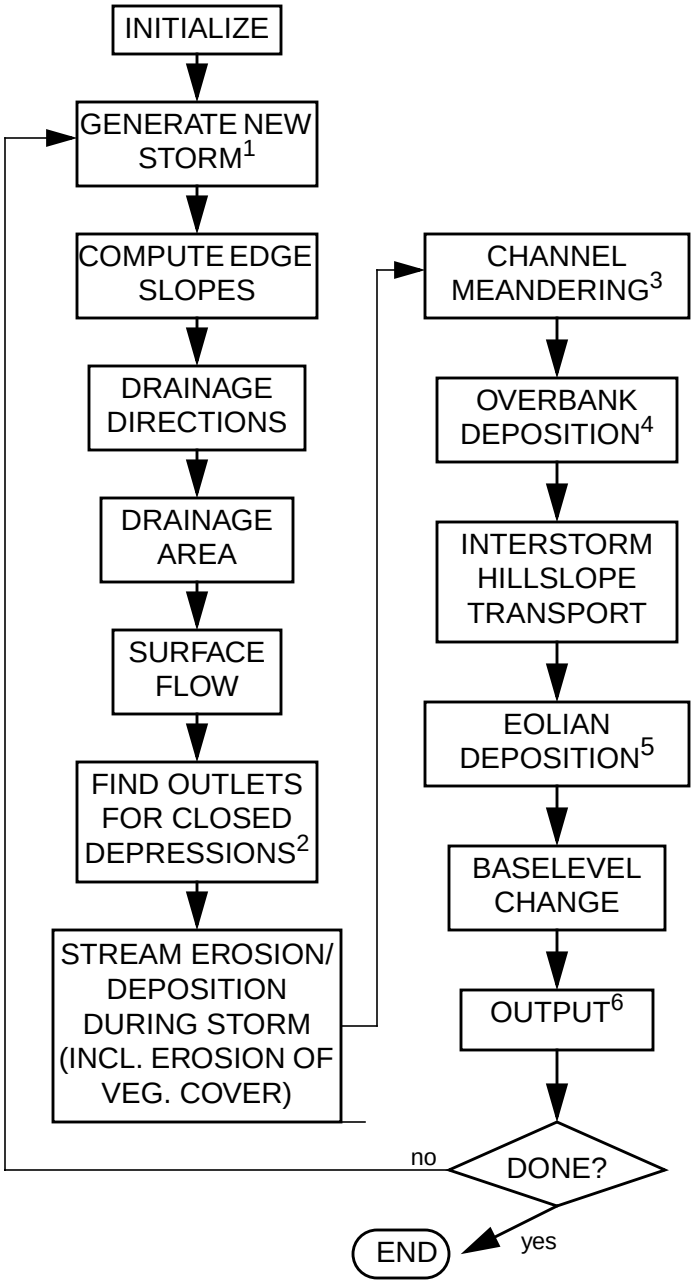

Notes:

1. If option for stochastic storms is selected; otherwise, mean storm properties are used.
2. If the option for lake-filling is selected; otherwise, flow entering a closed depression is assumed to evaporate.
3. If the meandering option is selected.
4. If option selected.
5. If option selected.
6. At selected intervals.

FIGURE 2. Flow chart showing the sequence of computations in the model.

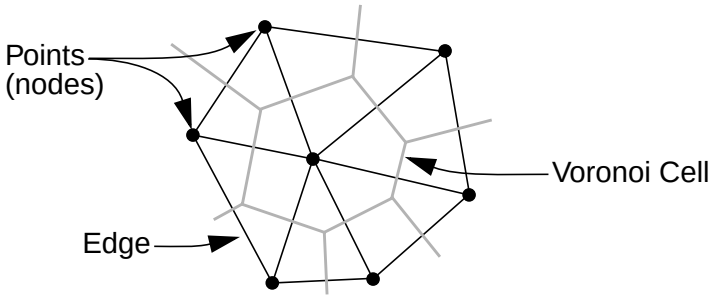

FIGURE 3. Schematic illustration of model grid components.

Voronoi cell has surface area Λ.

CHILD's mesh-handling routines include the capability of either reading in an existing mesh (e.g., from a previous simulation or as output from a GIS system), or creating a new mesh. Meshes can be created from a given set of points or from an input gridded DEM in Arc/Info GRID format (in which case the elevations of the points are interpolated). Alternatively, a "synthetic" rectangular domain can be created, using either a uniform (hexagonal) triangulation, a "perturbed" uniform triangulation in which the horizontal position of each point is offset by a random amount, or a triangulation constructed from a collection of randomly-distributed points.

CHILD's mesh-handling routines are also designed to allow for dynamic point addition, movement, and deletion while preserving the Delaunay criterion. This capability is what makes it possible to incorporate lateral stream channel erosion within floodplains. The data structures and algorithms used to implement the TIN mesh are discussed in Section I-C. Section II-B presents further details on the use of dynamic remeshing to model stream meandering.

Climate Module

Each model iteration represents a storm event. Each storm event is associated with a rain-

fall (or runoff) intensity, P, a duration, T_r, and an interstorm period before the next event, T_b. These parameters may be chosen at random for each storm using the model of Eagleson (1978), or they may be held constant throughout a simulation. In either case, storms are approximated as having constant rainfall intensity throughout their duration, and the same assumption is applied to the resulting hydrographs (see below).

For variable storms, the storm properties are chosen at random from the following distributions:

Rainfall (runoff) intensity $$f(P) = \frac{1}{\bar{P}} \exp\left(-\frac{P}{\bar{P}}\right) \quad (2)$$

Storm duration $$f(T_r) = \frac{1}{\overline{T_r}} \exp\left(-\frac{T_r}{\overline{T_r}}\right) \quad (3)$$

Interstorm period $$f(T_b) = \frac{1}{\overline{T_b}} \exp\left(-\frac{T_b}{\overline{T_b}}\right) \quad (4)$$

where $\bar{P}$, $\overline{T_r}$, and $\overline{T_b}$ are mean storm intensity, duration, and interstorm period, respectively. If stochastic storm generation is not used, the mean values are applied during each iteration (in which case the total duration of each iteration is $\overline{T_r} + \overline{T_b}$). To model long-term variations in mean climate (such as late-Quaternary climate variations), the parameters $\bar{P}$, $\overline{T_r}$, and $\overline{T_b}$ may be varied sinusoidally with time over a given period of forcing. Note that for computational efficiency, storm and interstorm durations can be increased. As long as their ratio remains the same, the distribution of event magnitudes is preserved.

Flow Routing and Runoff

Surface flow collected at a point on the mesh is routed downslope toward one of its adja-

cent neighbor nodes, following the edge that has the steepest downhill slope. If a pit occurs on the mesh, with no downhill route away from a given node, water is either assumed to evaporate at that point, or a lake-filling algorithm is invoked to find an outlet for the closed depression (see Section I-C).

The local contribution from rainfall at a node is equal to the effective runoff rate times the node's Voronoi area, Λ. The drainage area, A, for a node is the sum of the area of all Voronoi cells that contribute flow to that node. Surface discharge can be computed from drainage area in one of the following ways:

1. Hortonian (infiltration-excess) runoff: Runoff production (rainfall minus infiltration) is assumed to be uniform across the landscape. Assuming steady-state flow, the surface discharge at any point is equal to

$$Q = (P - I_c)A, \tag{5}$$

where I_c is infiltration capacity ($Q = 0$ if $P < I_c$).

2. "Bucket" runoff: The soil, canopy and surface are collectively assumed to have a finite and spatially uniform capacity to absorb rainfall. Any rainfall exceeding this storage depth will contribute to runoff according to

$$R = \frac{T_r P - D_{sr}}{T_r}, \tag{6}$$

where R is local runoff rate (L/T), D_{sr} is the soil-canopy-surface retention depth, and the resulting discharge at any point is $Q = RA$. Note that equation (6) describes a runoff rate that is constant throughout a storm and equal to the total volume of excess rainfall divided by the storm duration. Note also that $R = 0$ if $D_{sr} > T_r P$.

3. Modified O'Loughlin (1986) saturation-excess runoff model: Rainfall is partitioned between overland and shallow subsurface flow. The capacity for shallow subsurface flow per unit contour length is assumed to depend on local slope and soil transmissivity,

$$\frac{Q_{ss}}{w_v} = TS, \tag{7}$$

where in the model contour length is represented by the width of adjoining Voronoi cell edges, w_v (see Section IC). The surface flow component is equal to the total discharge minus the amount that travels in the subsurface,

$$Q = PA - TSw_v, \qquad PA > TSw_v. \tag{8}$$

Here, Q represents discharge resulting from a combination of saturation-excess overland flow and return flow. Note that this method assumes hydrologic steady-state for both surface and subsurface flows, and thus is most applicable to prolonged storm events.

4. Modified TOPMODEL scheme (Beven and Kirkby, 1979; Ijjasz-Vasquez et al., 1992): This approach is similar to method #3 above, but differs in that return flow is not modeled. Only saturation-excess rainfall contributes to surface runoff (infiltrated rainfall is assumed to contribute only to baseflow, and is therefore ignored). The model assumes a uniform infiltration capacity, I_c. The infiltration-excess component of runoff is

$$R_{ix} = P - I_c, \qquad P > I_c. \tag{9}$$

Soils are assumed to have a moisture storage capacity (saturation deficit) that depends on contributing area per unit contour length and on local topographic gradient,

$$S_c = \ln\left(\alpha \frac{A}{S w_v}\right). \quad (10)$$

As in method #3 contour width is represented by Voronoi cell width w_v. The parameter α determines the size of the soil moisture deficit per unit area and gradient. The saturation-excess component of runoff at a site is equal to the excess rainfall divided by the storm duration,

$$R_{sat} = \frac{(P - R_{ix})T_r - S_c}{T_r}, \qquad (P - R_{ix})T_r > S_c \quad . \quad (11)$$

The total runoff at a site is equal to the sum of the infiltration-excess and saturation-excess components,

$$R = R_{ix} + R_{sat} \ , \quad (12)$$

and the total discharge at a site is equal to the sum of runoff generated at each upstream site,

$$Q_i = \sum_{j=1}^{n} R_j, \quad (13)$$

where *j* represents nodes that drain to node *i*.

These four alternative runoff-generation models are simplistic, but they have the advantages of being computationally efficient and of allowing the user to choose a method that is appropriate to the environment of interest.

Hillslope Sediment Transport

Sediment transport by “continuous” hillslope processes such as soil creep and raindrop impact is modeled using the well-known geomorphic diffusion equation (e.g., Culling, 1960),

$$\left.\frac{\partial z}{\partial t}\right|_{\text{creep}} = k_d\left(\frac{\partial^2 z}{\partial x^2} + \frac{\partial^2 z}{\partial y^2}\right). \quad (14)$$

Numerical solution of equation (14) on an irregular mesh is discussed in Section IC. In addition, a module for landsliding presently exists within the GOLEM model (Tucker and Bras, 1998), and will be incorporated into CHILD in a future update.

Hydraulic Geometry

In the formulation for erosion and deposition (see below), information on channel properties such as width, depth, and roughness is essentially lumped into a single transport or detachment coefficient. However, information about channel depth, width, and/or roughness may still be needed in three cases: (1) if the stream meandering option is used, channel width, depth and roughness are needed for any “meandering nodes” (nodes possessing a high enough discharge that meandering is activated; see below); (2) bankfull channel depth is needed in order to compute overbank deposition when this option is used; (3) if landscape material is not vertically homogeneous, bankfull channel depth is used to compute the (a) the depth over which sediment properties (grain size composition) are averaged in calculating transport capacity, and (b) the depth of the material that effectively controls detachment capacity. In each case, channel properties are computed using the well-known empirical relationships defined by Leopold and Maddock (1953). The magnitude of a bankfull runoff event, R_b, is used as an input parameter.

Stream Erosion and Deposition

The model distinguishes between detachment of material from a stream bed and transport of the detached material. The maximum detachment rate depends on local slope and discharge according to

$$D_b = k_b(k_t Q^{m_b} S^{n_b} - \theta_{cb})^{p_b}, \quad (15)$$

where D_b is the detachment (erosion) rate, θ_{cb} is a threshold, and k_b, k_t, m_b, n_b, and p_b are parameters. Note that with suitably chosen parameters, equation (15) can represent excess shear stress, with $D_b = k_b(\tau - \tau_{cb})^{p_b}$ (τ = bed shear stress, τ_{cb} = critical shear stress for erosion) (Whipple and Tucker, 1999). This basic formulation is similar to that used in the WEPP (Foster and Meyer, 1972; Foster et al., 1995) and SIMWE (Mitas and Mitasova, 1998) soil erosion models as well as in the drainage basin evolution models of Howard (1994) and Tucker and Slingerland (1997).

The transport capacity for detached sediment material of a single grain size is

$$C_s = W k_f(k_t Q^{m_f} S^{n_f} - \theta_c)^{p_f}, \quad (16)$$

where C_s is transport capacity (L^3/T), W is channel width, and k_f, k_t, m_f, n_f, and p_f are parameters. As with equation (15), equation (16) can be expressed in terms of excess bed shear stress using suitably-chosen values for k_f, m_f, and n_f. In the present version of the model, channel width is computed using the empirical relationship $W = k_{cw} Q^{m_{cw}}$ (the constant k_{cw} is assumed to be absorbed into the transport coefficient k_f).

Two end-member cases and one intermediate case arise from equations (15) and (16); for computational efficiency, a special subroutine is provided in the model to handle the first of these

cases separately:

Detachment-limited: If the sediment transport capacity is everywhere greater than the sediment flux, the rate of water erosion is simply equal to the maximum detachment rate,

$$\frac{\partial z_b}{\partial t} = -D_c, \tag{17}$$

where z_b represents elevation of the channel bed above a datum within the underlying rock column. This formulation has been used in a number of studies to represent bedrock channel erosion (or more generally, detachment-limited erosion) (e.g., Seidl and Dietrich, 1992; Anderson, 1994; Howard et al., 1994; Seidl et al., 1994; Tucker and Slingerland, 1994, 1996, 1997; Moglen and Bras, 1995). It has the practical advantage of being simple and efficient to integrate numerically.

Transport-limited: If sufficient sediment is always available for transport and/or the bed material is easily detached, streams can be assumed to be everywhere at their carrying capacity. Under this condition, continuity of mass gives the local rate of erosion or deposition as

$$\frac{\partial z_b}{\partial t} = -\frac{1}{\rho_s}\frac{\partial C_s}{\partial \hat{x}}, \tag{18}$$

where ρ_s is sediment bulk density and $\hat{x}$ is a vector oriented in the direction of flow (note that usually the bulk density term is absorbed into the transport coefficient).

The first of these cases can be invoked in the model by selecting the “detachment-limited” stream erosion option. Alternatively, the model may be run in “detachment-transport” mode. This represents the most general case. In detachment-transport mode, the rate of erosion is computed as the lesser of (1) the excess sediment carrying capacity or (2) the maximum detachment rate.

Detachment capacity can be specified separately for regolith and bedrock material (cf. Howard, 1994).

Entrainment of Transport of Multiple Sediment Sizes

Version 2.0 of the CHILD model is designed to simulate transport of sand and gravel sediment fractions, using the transport model developed by Wilcock (1997, 1998). Details on the multi-size transport model can be found in sections I-F, III-B, and III-C. Note that with the introduction of variable subsurface stratigraphy, it becomes important to define the effective depth over which landscape materials are subjected to erosion. The effective depth of erosion is taken as equal to the local channel depth, which is modeled using a simple empirical relationship (see Hydraulic Geometry, above). If multiple sediment layers are exposed, the effective sediment composition is taken as a weighted average over the depth of the channel.

Stratigraphy

When sediment is deposited, CHILD keeps track of the properties of the deposited material through the use of a “layering” module. Sediment properties tracked within each layer include the date of most recent deposition, grain size composition, detachment coefficient, surface exposure age (see Geoarchaeology and Surface Exposure Age-Tracking, below), and a flag indicating whether the material is considered regolith or bedrock. Layers may be of any thickness, subject to two constraints: (1) an active layer of constant thickness is always maintained at the surface, except when bedrock is exposed; and (2) when new material is transferred from the active layer to the underlying layer as a result of deposition, the thickness of the “receiving” layer cannot exceed that of the active layer; whenever this maximum thickness is reached, a new layer is created. When material is “mixed” into an existing layer, the properties of the new layer are found by com-

puting a weighted average. The total number of layers may vary from node to node, and is limited only by memory resources. When points are moved or added, an interpolation procedure is used to update the thickness and composition of layers, with strata correlated on the basis of age. Example applications that make use of the model's stratigraphy capabilities are presented in Sections I-F, I-G, and II-C. The stratigraphy model was originally developed as a prototype within the framework of the GOLEM model; applications of this prototype are discussed in Sections III-B and III-C.

Geoarchaeology and Surface Exposure Age-Tracking

For geoarchaeological applications, the present version of the CHILD model includes the ability to track an effective surface exposure age associated with each sediment layer at each node. The exposure age of a deposit represents the length of time the material spent at or near the surface (more precisely, it represents the total duration over which the material lay within a distance L_a of the surface, where L_a is the depth of the active layer). These exposure ages can be combined with a probabilistic model for deposition of cultural material in order to generated simulated space-time maps of archaeological resource potential. Application of these capabilities is discussed in Section II-C.

Lateral Stream Channel Erosion (Meandering)

In order to enable the model to serve as a tool for exploring the dynamics of floodplain evolution, the present version of CHILD includes a link to a 1D model of stream meandering. The theory behind the stream meander model is described in Sections II-A and II-B. Coupling of the model with CHILD is discussed in Section II-B, and an example application to floodplain stratigraphy and geoarchaeology is presented in Section III-C.

Floodplain Overbank Deposition Module

The method for simulating flow erosion and sediment transport described above does not generally apply to overbank flows during flooding events. To simulate the effects of deposition during overbank flood events on alluvial stratigraphy, CHILD includes a module to simulate overbank deposition using a modified form of the diffusion model of Howard (1992). The model was developed for application to drainage basins in which the alluvial stratigraphic record consists primarily of overbank fines, as for example in the case of low-relief drainage basins in and around Fort Riley, Kansas (Johnson, 1998). In the modified overbank deposition model, the deposition rate during a flood depends on distance from a main channel and on local flood depth,

$$D_{OB} = (W - z)\mu \exp(-d/\lambda) \tag{19}$$

where D_{OB} is the vertical deposition rate, z is local elevation, d is the distance between the point in question and the nearest point on the main channel, W is the water surface height at the nearest point on the main channel, μ is a deposition rate constant, and λ is a distance-decay constant. "Main channel" is defined on the basis of a drainage area threshold; typically, however, the model would be configured with a large channel fed in as a boundary condition, so that there would be no ambiguity about what constitutes a primary channel (see Section II-C). Equation (19) is only applied for events that surpass a given threshold rainfall intensity; smaller events are assumed not to generate significant overbank flooding.

Eolian Deposition Module

During much of the Quaternary, deposition of fine sediment (loess) by wind has been a significant geomorphic process in many parts of the world. The most spectacular example is the Loess Plateau in China, where loess accumulations of up to hundreds of meters in thickness occur.

The U.S. midcontinent is also an area of significant loess accumulation, and the process of episodic loess deposition appears to have had an important impact on the preservation of the prehistoric archaeological record and on the dynamic response of catchments to climate change (e.g., Johnson and Logan, 1990; Johnson, 1998). To address such issues, CHILD includes a simple eolian deposition module. The model is based on a spatially and temporally uniform rate of loess deposition at a rate D_L. The layering module makes it possible to track the stratigraphic consequences of loess input. An example application of the eolian deposition module is discussed in Section II-G.

References

Ahnert, F., 1976, Brief description of a comprehensive three-dimensional process-response model of landform development: Zeitschrift fur Geomorphologie, v. 25, 29-49, 1976.

Anderson, R.S., 1994, Evolution of the Santa Cruz Mountains, California, through tectonic growth and geomorphic decay: Journal of Geophysical Research, v. 99, p. 20,161-20,179.

Beven, K.J., and Kirkby, M.J., 1979, A physically based variable contributing area model of basin hydrology: Hydrological Sciences Bulletin, v. 24, no. 1, p. 43-69.

Culling, W.E.H., 1960, Analytical theory of erosion: Journal of Geology, v. 68, p. 336-344.

Eagleson, P.S., 1978, Climate, soil, and vegetation: 2. the distribution of annual precipitation derived from observed storm sequences: Water Resources Research, v. 14, p. 713-721.

Foster, G.R., Flanagan, D.C., Nearing, M.A., Lane, L.J., Risse, L.M., and Finkner, S.C., 1995, Chapter 11: Hillslope erosion component, in USDA-Water Erosion Prediction Project, National Soil Erosion Research Laboratory Report No. 10, p. 11.1-11.12 (http://soils.ecn.purdue.edu/~wepphtml/wepp/wepptut/ahtml/doc.html).

Foster, G.R., and Meyer, L.D., 1972, A closed-form erosion equation for upland areas, in Shen, H.W., ed., Sedimentation: Symposium to Honor Professor H. A. Eninstein, p. 12.1-12.19, Colorado State University, Fort Collins, CO.

Howard, A.D., 1992, Modeling channel and floodplain sedimentation in meandering streams, in Lowland Floodplain Rivers: Geomorphological Perspectives, John Wiley & Sons, Chichester, United Kingdom, p. 1-41.

Howard, A.D., 1994, Badlands, in Abrahams, A.D., and Parsons, A.J., eds., Geomorphology of desert environments: London, Chapman and Hall, p. 213-242.

Howard, A.D., Dietrich, W.E., and Seidl, M.A., 1994, Modeling fluvial erosion on regional to continental scales: Journal of Geophysical Research, v. 99, p. 13,971-13,986.

Ijjasz-Vasquez, E.J., Bras, R.L., and Moglen, G.E., 1992, Sensitivity of a basin evolution model to the nature of runoff production and to initial conditions: Water Resources Research, v. 28, p. 2733-2741.

Johnson, W.C., 1998, Paleoenvironmental Reconstruction at Fort Riley, Kansas, 1998 Phase,

Technical Report submitted to U.S. Army Construction Engineering Research Laboratory.
Johnson, W.C., and Logan, 1990, Geoarchaeology of the Kansas River Basin, central Great Plains, in Lasca, N.P., and Donohue, J., eds., Archaeological Geology of North America: Geological Society of America, Decade of North American Geology Centennial Special Volume 4, p. 267-299.
Kirkby, M.J., 1987, Modelling some influences of soil erosion, landslides and valley gradient on drainage density and hollow development: Catena Supplement, v. 10, p. 1-14.
Mitas, L., and Mitasova, H., 1998, Distributed soil erosion simulation for effective erosion prevention: Water Resources Research, v. 34, p. 505-516.
Moglen, G.E., and R.L. Bras, 1995, The Effect of Spatial Heterogeneities on Geomorphic Expression in a Model of Basin Evolution, Water Resources Research v. 31, no. 10, p. 2613-23.
O'Loughlin, E.M., 1986, Prediction of surface saturation zones in natural catchments: Water Resources Research, v. 22, p. 794-804.
Seidl, M.A., and Dietrich, W.E., 1992, The problem of channel erosion into bedrock: Catena Supplement 23, p. 101-124.
Seidl, M.A., Dietrich, W.E., and Kirchner, J.W., 1994, Longitudinal profile development into bedrock: an analysis of Hawaiian channels: Journal of Geology, v. 102, p. 457-474.
Tucker, G.E., and Bras, R.L., 1998, Hillslope processes, drainage density, and landscape morphology: Water Resources Research, v. 34, p. 2751-2764.
Tucker, G.E., Lancaster, S.T., Gasparini, N.M., Bras, R.L., and Rybarczyk, S.M., 1999, An object-oriented framework for distributed hydrologic and geomorphic modeling using triangulated irregular networks: submitted to Computers and Geosciences.
Tucker, G.E., and Slingerland, R.L., 1994, Erosional dynamics, flexural isostasy, and long-lived escarpments: a numerical modeling study: Journal of Geophysical Research, v. 99, p. 12,229-12,243.
Tucker, G.E., and Slingerland, R.L., 1996, Predicting sediment flux from fold and thrust belts: Basin Research, v. 8, p. 329-349.
Tucker, G.E., and Slingerland, R.L., 1997, Drainage basin response to climate change: Water Resources Research, v. 33, no. 8, p. 2031-2047.
Whipple, K.X., and Tucker, G.E., 1999, Dynamics of the stream power river incision model: implications for height limits of mountain ranges, landscape response timescales and research needs: J. Geophys. Res., in press.
Wilcock, P., 1997, A method for predicting sediment transport in gravel-bed rivers: Technical report for the U.S. Forest Service Rocky Mountain Forest and Range Experiment Station, 59 pp.
Wilcock, P., 1998, Two-fraction model of initial sediment motion in gravel-bed rivers: Science, v. 280, p. 410-412.
Willgoose, G.R., Bras, R.L., and Rodriguez-Iturbe, I., 1991, A physically based coupled network growth and hillslope evolution model, 1, theory: Water Resources Research, v. 27, p. 1671-1684.